# Thiolate-Imidazolium Ion Pair Is Not an Obligatory Catalytic Entity of Cysteine Peptidases: The Active Site of Picornain 3C†

Zsuzsa Sárkány, Zoltán Szeltner, and László Polgár*

*From the Institute of Enzymology, Biological Research Center, Hungarian Academy of Sciences, P. O. Box 7, H-1518 Budapest, Hungary*

*Received March 16, 2001; Revised Manuscript Received June 5, 2001*

ABSTRACT: Cysteine peptidases are thought to attack the substrate by a thiolate-imidazolium ion-pair, as demonstrated with the most extensively studied papain. Picornavirus proteinases (picornains), a different family of cysteine peptidases, are structurally related to the trypsin family of serine peptidases, whose catalytically competent histidine operates as a general base catalyst. Measuring the absorbance change upon alkylation of picornains at 250 nm, where the nondissociated thiol group has a negligible absorbance relative to the ionized form, one can test the ionization state of the catalytic cysteine. For such studies, we have prepared and used a mutated variant of the poliovirus proteinase 3C, which contains a single thiol group. The pH dependence of the molar extinction coefficient has undoubtedly shown that picornain 3C contains an ordinary thiol group rather than the usual ion-pair. Therefore, the imidazole assistance, demonstrated in alkylation reactions, is presumably general base catalysis, as found with serine peptidases. Kinetic studies on $k_{cat}/K_m$ gave large inverse deuterium isotope effects, which may overcompensate the reverse values characteristic of the potential general base catalysis. The inverse effects is associated with the stabilization of the protein structure in heavy water.

Picornaviruses are small icosahedral viruses, which constitute a large family of single-stranded positive-sense RNA viruses. They cause a wide variety of diseases in humans and animals, like common cold, hepatitis A, foot-and-mouth disease and poliomyelitis. The mRNA-like genome of picornaviruses is translated in the host cell into a large polyprotein, which is then cleaved by specific viral proteinases into structural and nonstructural proteins (*1*−*4*). In entero- and rhinoviruses, the 2A and 3C proteins process the polyproteins. Most cleavages are mediated by the larger 3C proteinase, designated picornain 3C. However, processing on the polyprotein is initiated by picornain 2A, which cleaves between the C-terminus of VP1 and its own N-terminus. This cleavage, the only one in fact carried out by picornain 2A, separates the capsid protein precursor from the noncapsid protein precursor. In addition to this cleavage, picornain 2A cleaves the cellular protein eukaryotic initiation factor 4G, which serves to down-regulate the translation of capped host cell mRNAs. Viral protein synthesis is unaffected as it initiates internally at an internal ribosomal entry site. The cleavage sites recognized by the rhinovirus and enterovirus picornains 2A are characterized by a P1′ glycine and preferences for P2 threonine, serine, or asparagine and P2′ proline or phenylalanine. Picornains 3C prefer a glutamine residue in the P1 position of the substrate. The major determinant of the specificity is a conserved histidine in the S1 pocket of the enzyme, and this residue (His161 in poliovirus proteinase 3C) donates a hydrogen bond to the carbonyl oxygen of the side chain of the glutamine. Besides their processing function, picornains 3C possess an RNA binding site, which is probably required for the initiation of RNA replication (*4*).

The structures of picornains 2A and 3C show a marked relationship to serine peptidases, despite the fact that they are cysteine peptidases. This feature warranted their grouping in a new family of cysteine peptidases, namely family C3 in clan CB. The three-dimensional structures of the picornains 3C from hepatitis A virus (*5*), rhinovirus (*6*), and poliovirus (*7*) have been determined, while that of the first picornain 2A (HRV2) has been recently solved (*8*). It is clear from the three-dimensional structure that the catalytic triad of HRV2 proteinase 2A involves Cys106, His18, and Asp 35, while the catalytically competent groups of poliovirus proteinase 3C are Cys147, His40, and Glu71. Accordingly, picornains differ from the most extensively studied cysteine peptidases of the papain family, which contain an asparagine residue as the third member of the catalytic triad, while picornains have a charged residue, Asp35 in HRV2[1] proteinase 2A and Glu71 in poliovirus proteinase 3C. In this respect, picornains resemble the enzymes of the chymotrypsin family, which also have a carboxyl group in the catalytic triad. It is therefore an intriguing question whether the reactive nucleophile of picornains is the thiolate ion of

† This work was supported by the Hungarian Science Fund (OTKA T/9 T022808).

* To whom correspondence should be addressed. Phone: 36-1-466-5633. Fax: 36-1-466-5465. E-mail: polgar@enzim.hu.

[1] Abbreviations: HRV2, human rhinovirus type 2; PV3C, poliovirus picornain 3C; PV3C(M27G), Met27Gly variant of poliovirus picornain 3C; PV3C(M27G/C153S), doubly mutated poliovirus picornain 3C; EDTA, ethylenediaminotetraacetic acid; Mes, 2-(morpholino)ethanesulfonic acid; Abz, 2-aminobenzoic acid; DTE, dithioerithritol; Phe-($NO_2$), 4-nitrophenylalanine; $Nbs_2$, 5.5′-dithio-bis(2-nitrobenzoic acid); DSC, differential scanning calorimetry.

10.1021/bi010550p CCC: $20.00 
Published on Web 08/10/2001

a thiolate-imidazolium ion pair, as found with papain (*9*, *10*) or the reaction of the nondissociated thiol group is facilitated by general base catalysis by the catalytic histidine, which mechanism is prevalent with serine peptidases using the OH group of the active site serine residue to attack the substrate carbonyl carbon atom.

We have recently reported that the pH dependence of the alkylation of picornain 2A of HRV2 shows two reactive thiol forms, namely the free thiolate ion at high pH, and an imidazole assisted thiol group in the active, lower pH range (*11*). However, the results did not permitted to distinguish between the two possible mechanisms: nucleophilic attack by the thiolate-imidazolium ion-pair and general base catalysis by the imidazole group. The existence of an ionized thiol group can be uncovered by the spectrophotometric method, we have developed earlier to show the thiolate ion of papain and thiolsubtilisin (*12*). Unfortunately, additional thiol groups, besides the catalytically competent one, interfere with the spectrophotometric method. Thus, picornain proteinase 2A, which contains seven thiol groups in total, did not seem to be suitable for such investigations. Instead, we have chosen poliovirus proteinase 3C which have only one extra thiol (Cys153) besides the active site thiol group (Cys147). The catalytically not influential extra thiol group can be eliminated by substituting a serine for the Cys153. The results have shown that, in distinction from papain, a thiolate-imdazolium ion-pair is not detectable in PV3C.

## EXPERIMENTAL PROCEDURES

*Preparation of PV3C*. The gene of PV3C was excised from the plasmid pExc (*13*, *14*) by the PCR method, using a primer (5′-CAGAACCATGGGGCCAGGGTTCGA-3′) to the 5′-end of the gene with NcoI restriction site (underlined), and another primer (5′-CGGGATCC*TTA*ATTGACTCTGAGTGAAG-3′) to the 3′-end with a *Bam*HI restriction site (underlined) and stop codon (italic). The amplified gene was digested with *Nco*I and *Bam*HI restriction endonucleases in the same reaction mixture, and ligated into the pTrc99A expression vector. The enzyme was produced in *Escherichia coli* JM105 with high yield. However, this construction yielded the proteinase 3C practically as inclusion bodies including a mixture of the complete enzyme with 183 amino acids, and a shorter truncated product beginning with Met27. A Shine-Dalgarno-like sequence and an inner initiation codon (ATG for Met27) was responsible for the production of the truncated picornain 3C (*14*). To eliminate the inner initiation codon, the ATG triplet of Met27 was changed to GGG coding for Gly, using the sense and antisense primer pair in the PCR method. One G was also changed to A in order to create an *Eco*RI restriction site (underlined), which renders it possible to verify the mutation by digestion.

Sense primer:
5′-ACTAGCAAGGGAGAaTTCACTggGTTAGGAGTCC-3′

Antisense:
3′-TGATCGTTCCCTCTtAAGTGAccCAATCCTCAGG-5′

In the first step of PCR, two independent reactions were carried out, using the Vent polymerase, the pTrc/3C plasmid as template digested with *Bam*HI enzyme. To this mixture was added the 5′-primer and the antisense mutagenic primer in the first reaction, and in the second reaction the 3′-primer and the sense mutagenic primer, 25 cycles in each run. The mutated gene was then obtained in two pieces, which were isolated by agarose gel electrophoresis. This was followed by purification with the QIAquick Gel Extraction Kit. In the second step the mixture of the two gene fragments were used as templates in the reaction mixture, heated to 95 °C prior to the addition of the Vent polymerase. The temperature was then lowered to 50 °C when the complementary ends of the two DNA portions formed double stranded DNA. Heating at 72 °C for 2 min allowed to proceed the synthesis of the complementary strands. The complete strands were able to bind the terminal primers (5′ and 3′ primers to the 5′ and 3′ termini of the gene, respectively), which were added to the mixture at 95 °C. The amplification was then carried out in 30 cycles at 95, 55, and 72 °C for 1, 1, and 0,6 min, respectively. The PCR product was identified on an agarose gel (2%) and purified with a QIAquick kit. The pure product was digested with *Nco*I and *Bam*HI restriction enzymes and isolated with agarose gel electrophoresis. After purification from the gel, it was ligated at 20 °C for 30 min into the pET3d vector digested by *Nco*I and *Bam*HI. The ligation mixture was transformed to *E. coli* DH5α. The plasmids were isolated from the colonies grown on LB, and tested for the insert by digestion with *Nco*I and *Bam*HI. *E. coli* BL21-(DE3)pLysE was transformed with the plasmid bearing the insert. This construction provided 28−30 mg/L of correctly folded enzyme in soluble form.

*Expression and Purification of PV3C Variants*. *E. coli* BL21(DE3)pLysE was used to express PV3C(M27G). Cells were grown in four 2000 mL flasks, each containing 500 mL of LB, at 37 °C to an OD of 0.5−0.6 at 600 nm. Isopropyl-$\beta$-D-thiogalactopyranoside (0.4 mM) and 50 $\mu$g/mL ampicillin were added and the incubation continued at 30 °C for about 15 h. The cells were harvested by centrifugation, suspended in 100 mL buffer (50 mM Tris-HCl, pH 7.5, 25 mM NaCl, 1 mM EDTA, 5 mM 2-mercaptoethanol, and 5% glycerol) and sonicated.

The cell extract was centrifuged for 30 min at 18000*g* and applied to a phosphocellulose column (2.7 × 20 cm) equilibrated with 50 mM Tris-HCl, pH 7.5, 1 mM EDTA, 5 mM 2-mercaptoethanol, and 5% glycerol (equilibration buffer). After washing with one column volume of equilibration buffer, the enzyme was eluted with a linear salt gradient (300 mL of equilibration buffer, and 300 mL of 0.5 M NaCl in the equilibration buffer). Active fractions eluted from the phosphocellulose column were combined (86 mL) and concentrated by ultrafiltration on an Amicon PM 10 membrane to 16.5 mL.

An aliquot (2 mL) of the concentrated solution was applied to a Sephacryl S100 column (1.6 × 118 cm) and eluted at a flow rate of 10 mL/h with 50 mM Tris-HCl buffer, pH 7.5, containing 1 mM EDTA, 100 mM NaCl, 5 mM 2-mercaptoethanol, and 5% glycerol. From 2000 mL of broth, 36.5 mg of PV3C(M27G) was obtained, with a $k_{cat}/K_m$ of 2193 $M^{-1}$ $s^{-1}$. The enzyme concentration was calculated from the absorbance at 280 nm by using $M_r$ value of 20 000 and $A_{280}$ (0.1%) of 0.42 (*15*). The enzyme was frozen under liquid nitrogen and stored at −70 °C.

The Cys153Ser mutation was introduced into the plasmid pET3d/PV3C/M27G by the same method as used for the Met27Gly mutation. The codon TGT of Cys153 was changed to AGT of Ser, and an A was also changed to T in order to

create a *Spe*I restriction site (underlined), which rendered it possible to verify the mutation by digestion. For introduction of the Cys153Ser mutation, the following primers were synthesized:

Sense primer:
5′-GAGTCATCACtaGTACTGGGAAAG-3′

Antisense: 3′-CTCAGTAGTGatCATGACCCTTTC-5′

The enzyme was expressed and purified as described for PV3C(M27G) and the specificity rate constant ($k_{cat}/K_m$) proved to be the same as for PV3C(M27G).

Active-site titration was carried out by measuring the thiol group concentration of the enzyme by titrating with $Nbs_2$ at pH 6.8 (*16*).

*Kinetic Measurements*. The activity of PV3C(M27G) was measured fluorometrically with the internally quenched substrate Abz-Glu-Ala-Leu-Phe-Gln-Gly-Pro-Phe($NO_2$)-Ala that is cleaved at the Gln-Gly bond. A sample (0.3 $\mu$L) of the substrate stock solution (1 mg/mL in dimethylformamide), was added to the reaction mixture of 1.0 mL final volume containing 40 mM Tris-HCl, pH 7.6, 1 mM EDTA, and 1 mM DTE. The substrate concentration (0.26 $\mu$M) was much below the $K_m$ value. Even the highest substrate concentration applied (175 $\mu$M) was still below the $K_m$. The reactions were started by the addition of enzyme (2−4 $\mu$M in the cell). Pseudo first-order rate constants obtained under these conditions were determined at 25 °C, using a Jasco FP 777 spectrofluorometer at 330 and 420 nm excitation and emission wavelengths, respectively. The second-order rate constant ($k_{cat}/K_m$) was calculated by dividing the pseudo first-order rate constant by the enzyme concentration.

The pH dependence of the rate constants was measured at 25 °C in a buffer containing 25 mM acetic acid, 25 mM Mes, 25 mM glycine, 75 mM Tris, 1 mM EDTA, and 1 mM DTE (standard buffer), adjusted to the required pH by the addition of 1 M NaOH or 1 M HCl. The data were fitted with the GraFit software (*17*) to the appropriate equations (eqs 1−3), where $k(\text{limit})_1$ and $k(\text{limit})_2$ are pH independent rate constants, and p$K_1$, p$K_2$, and p$K_3$ stand for the p$K_a$ values of catalytically competent functional groups.

$$k = k(\text{limit})_1[\text{l}/(\text{l} + 10^{\text{p}K_1-\text{pH}} + 10^{\text{pH}-\text{p}K_2})] + k(\text{limit})_2[\text{l}/(\text{l} + 10^{\text{p}K_2-\text{pH}})] \quad (1)$$

$$k = k(\text{limit})_1[\text{l}/(\text{l} + 10^{\text{p}K_1-\text{pH}} + 10^{\text{pH}-\text{p}K_2})] + k(\text{limit})_2[\text{l}/(\text{l} + 10^{\text{p}K_2-\text{pH}} + 10^{\text{p}K_2+\text{p}K_3-2\text{pH}})] \quad (2)$$

$$k = k(\text{limit})[\text{l}/(\text{l} + 10^{\text{p}K_1-\text{pH}} + 10^{\text{pH}-\text{p}K_2})] \quad (3)$$

The reaction of PV3C(M27G) with iodoacetamide or iodoacetate was followed under pseudo-first-order conditions by taking aliquots from the reaction mixture at appropriate times and by measuring the decrease in the enzymatic activity. The second-order rate constant was calculated by dividing the first-order rate constant by the concentration of the alkylating agent. The reaction mixture contained 0.10−0.13 mM enzyme in a buffer composed of 25 mM acetic acid, 25 mM Mes, 25 mM glycine, 75 mM Tris, 1 mM EDTA. and 1.4−3.0 mM iodoacetamide or 2.0−4.3 mM iodoacetate.

The molar extinction coefficient of the dissociated thiol group in PV3C(M27G/C153S) was determined at 250 nm by monitoring the absorbance change during alkylation as described in detail (*12*). Samples of 10.9−18.5 $\mu$M PV3C(M27G/C153S) was alkylated with 0.79 mM iodoacetate in 1 mL of buffer composed of 25 mM acetic acid, 25 mM Mes, 25 mM glycine, 75 mM Tris, and 0.2 mM EDTA at 25 °C.

Rate-limiting general base/acid catalysis was tested in heavy water (99.9%). The deuterium oxide contents of all reaction mixtures were at least 98%. The $p^2H$ of deuterium oxide solutions can be obtained from pH meter readings according to the relationship $p^2H$ = pH(meter reading) + 0.4 (*18*).

Unfolding of PV3C was determined by measuring the rate of fluorescence change in the standard buffer (pH 7.6) made from water and deuterium oxide, respectively, both containing 4.8 M urea. Unfolding was monitored at 25 °C and at 290 and 351 nm excitation and emission wavelengths, respectively.

Temperature dependence of the rate constants was determined at appropriate temperatures, using a thermostated cell holder. The reactions were started once the thermal equilibrium had been reached in the cell, which was controlled with a Digi-Sense thermometer (Cole-Palmer). Activation parameters were calculated from the linear plots of $\ln(k/T)$ versus $1/T$ (eq 5):

$$\ln(k/T) = \ln(R/N_A h) + \Delta S^*/R - \Delta H^*/RT \quad (5)$$

where $k$ is the rate constant, $R$ is the gas constant (8.314 J mol$^{-1}$ K$^{-1}$), $T$ is the absolute temperature, $N_A$ is the Avogadro number, $h$ is the Planck constant, the enthalpy of activation $\Delta H^*$ = −(slope) × 8.314 J mol$^{-1}$, the entropy of activation $\Delta S^*$ = (intercept − 23.76) × 8.314 J mol$^{-1}$ K$^{-1}$. The free energy of activation, $\Delta G^*$, was calculated from eq 6.

$$\Delta G^* = \Delta H^* - T\Delta S^* \quad (6)$$

Calorimetric measurements were carried out with a Microcal VP-DSC (Microcal Inc.) differential scanning calorimeter. Denaturation curves were recorded between 10 and 70 °C, at a pressure of 2.5 atm using a scan rate of 1 °C/min.

## RESULTS AND DISCUSSION

*Alkylation of PV3C(M27G)*. Picornains are structurally distinct from cysteine proteinases of the papain family. They are related to the chymotrypsin type enzymes both in their tertiary structure and in their catalytic triad which contains aspartic or glutamic acid rather than asparagine characteristic of the papain family. It is not clear, however, whether the catalytic histidine forms a thiolate-imidazolium ion-pair with the essential thiol group, as in papain, or it functions as a general base catalyst, as in chymotrypsin.

It has recently been shown that the imidazole facilitates the nucleophilic reaction of picornain 2A, in particular at neutral and slightly acidic pH, where an ordinary thiol group does not dissociate, and thus displays negligible nucleophilic reactivity (*11*). As for PV3C(M27G), similar behavior can be observed (Figure 1). Figure 1a shows the pH dependence

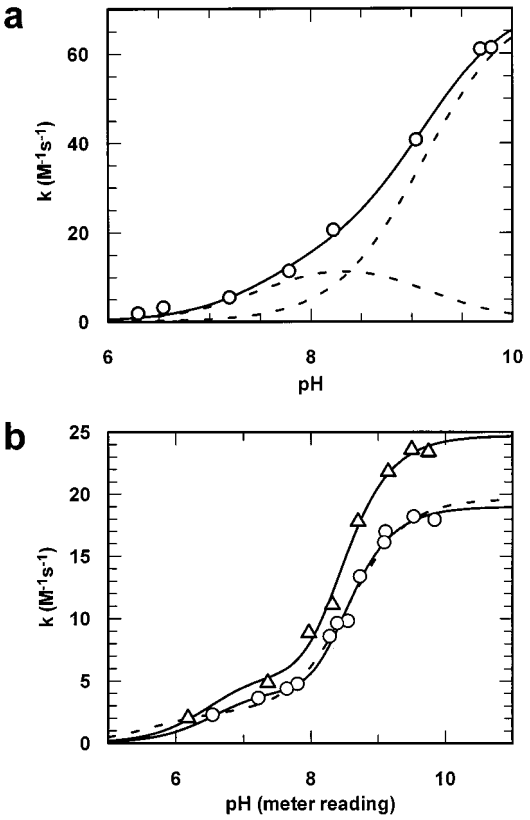


FIGURE 1: Second-order rate constants for alkylation of PV3C-(M27G). (a) The reactions were carried out with iodoacetamide. The data were fitted to eq 1 (solid line). The broken lines show the contribution of the two reactive enzyme forms. (b) The inactivation of the enzyme was performed with iodoacetate (○). The data were fitted to eq 1 (broken line) and eq 2 (solid line). The points marked with (△) signs were determined in 98% deuterium oxide and fitted to eq 2. The data measured in heavy water are discussed in section "Kinetic deuterium isotope effects".

Table 1: Kinetic Parameters for Alkylation of PV3C(M27G)

| | iodoacetamide | iodoacetate | | | |
|---|---|---|---|---|---|
| | eq 1 | eq 1 | eq 2 (A) | eq 2 (B)[a] | A/B |
| $k(\text{limit})_1$ ($M^{-1}$ $s^{-1}$) | 15.4 ± 4.4 | 2.4 ± 0.7 | 4.7 ± 1.0 | 6.0 ± 1.7 | 0.78 |
| $k(\text{limit})_2$ ($M^{-1}$ $s^{-1}$) | 71.8 ± 2.9 | 19.6 ± 0.6 | 19.0 ± 0.7 | 24.7 ± 0.9 | 0.77 |
| $pK_1$ | 7.54 ± 0.28 | 5.62 ± 2.2 | 6.61 ± 0.35 | 6.52 ± 0.40 | |
| $pK_2$ | 9.11 ± 0.13 | 8.55 ± 0.08 | 8.42 ± 0.17 | 8.40 ± 0.18 | |
| $pK_3$ | | | 8.24 ± 0.37 | 8.03 ± 0.48 | |

[a] Measured in 98% $^2H_2O$.

of the second-order rate constant of inactivation with iodoacetamide. The data conform to a complex ionization curve composed of bell-shaped and sigmoid terms (broken lines), representing the imidazole assistance, and the reaction of the free thiolate ion, respectively (eq 1).

With the charged iodoacetate the data do not exactly fit to eq 1 (broken line in Figure 1b). A better fitting is obtained once the contribution of an additional base has been taken into account (eq 2). The parameters of the curves are shown in Table 1. It may be noted that the error of $pK_1$ calculated with eq 1 is very large because the data could only be collected above $pK_1$. The nature of the extra base characterized by $pK_3$ is not known, and its contribution to the reaction with iodoacetate is not obvious. However, its participation may not be excluded since the data in Figure 1a also fit to

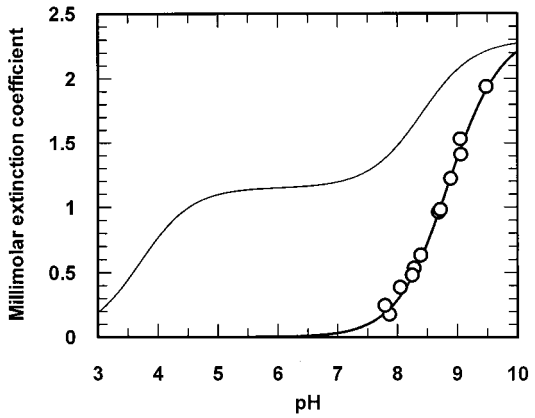


FIGURE 2: pH dependence of the molar extinction coefficient of Cys147 of PV3C(M27G) as calculated from the reaction with iodoacetate. The points were fitted to a simple sigmoid curve of the GraFit software (*17*) using the following parameters: $\epsilon = 2.37 \pm 8$ $mM^{-1}$ $cm^{-1}$, $pK_a = 8.86 \pm 0.03$. As a comparison, the change in the molar extinction coefficient for papain is shown by the thin line calculated with eq 1 when $\epsilon$ is substituted for $k$. $\epsilon(\text{limit})_1 = 1.15$ $mM^{-1}$ $cm^{-1}$, $\epsilon(\text{limit})_2 = 2.30$ $mM^{-1}$ $cm^{-1}$, $pK_1 = 3.7$, $pK_2 = 8.4$ (from ref *9*).

eq 2, so that they provide precisely the same curve as obtained with eq 1. The alkylation rate constants for the PV3C are several times higher than those found with the HRV2 picornain 2A (*11*).

*Ionization of the Catalytic Thiol Group.* It is generally agreed that in cysteine proteinases the catalytic assistance by the imidazole group is realized through the formation of a thiolate-imidazolium ion-pair (*4*). Evidence for the thiolate-imidazolium ion-pair, which rules out general base catalysis, can be obtained if a significant amount of the ionized thiol group of PV3C is found below pH 8 where the participation of the histidine is apparent, but the thiol group is generally not dissociated. The absorbance of the thiolate ion can be measured at 250 nm since at this wavelength the absorbance of the nondissociated form is negligible (*12*). The molar extinction coefficient of the thiolate ion was calculated from the absorbance difference measured before and after alkylation of the thiol group (*9*, *12*). Evidently, the formation of a covalent bond during alkylation abolishes the absorbance of the ionized form. For such measurements PV3C(M27G/C153S) was chosen since in this variant other thiol groups did not interfere with the determination of the active site Cys147. The other type of picornains, specifically HRV2 picornain 2A, may not be suitable because it contains seven cysteine residues. Disappearance of the absorbance of the thiolate ion of PV3C(M27G/C153S) was measured in the reaction with iodoacetate (Figure 2). Unexpectedly, the calculated molar absorbance of the thiolate ion perfectly conformed to a simple dissociation curve characteristic of Cys147. No deviation was found from the theoretical curve at low pH, where the thiolate-imidazolium ion-pair was expected to occur. Hence, in the catalytically competent pH range the probability of the occurrence of the thiolate-imidazolium ion-pair is negligible, less than the experimental error. This is a fundamental difference from papain (see Figure 2) and thiolsubtilisin because in these enzymes the absorbance of the thiolate ion of the ion-pair has clearly been demonstrated. In contrast, Figure 2 shows a simple ionization curve with a molar absorbance of 2370 $M^{-1}$ $cm^{-1}$, which well corresponds to the free thiolate ion of glutathione,

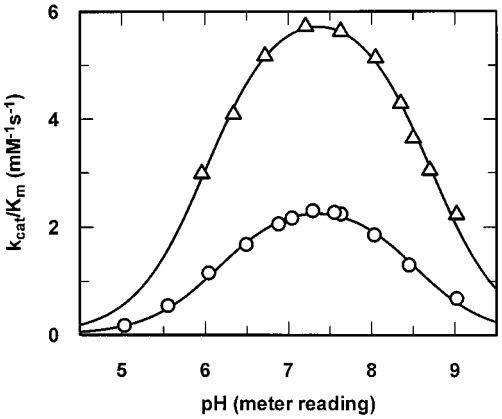


FIGURE 3: pH−$k_{cat}/K_m$ profile for the reaction of PV3C(M27G) with the oligopeptide substrate Abz-Glu-Ala-Leu-Phe-Gln-Gly-Pro-Phe($NO_2$)-Ala-OH. The points were fitted to eq 3 using the parameters $k_{cat}/K_m$(limit) = 2.55 ± 0.04 $mM^{-1}$ $s^{-1}$, p$K_1$ = 6.17 ± 0.03, p$K_2$ = 8.52 ± 0.04 (○). The same reactions performed in deuterium oxide are marked with (△) signs, and the parameters are $k_{cat}/K_m$(limit) = 6.23 ± 0.11 $mM^{-1}$ $s^{-1}$, p$K_1$ = 6.02 ± 0.03, p$K_2$ = 8.70 ± 0.03.

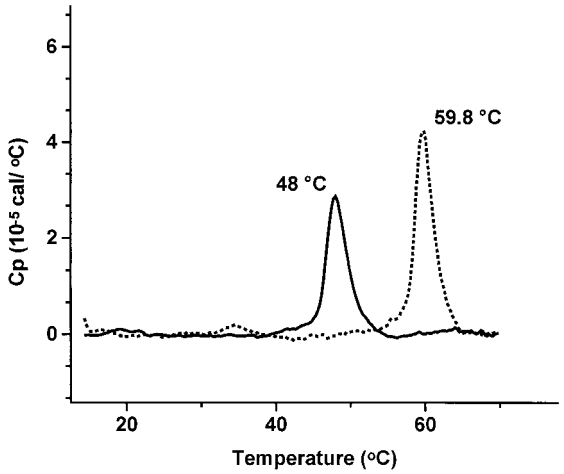


FIGURE 4: Calorimetric melting profiles of PV3C(M27G). Denaturation of the enzymes was measured in ordinary water (solid line) or heavy water (dotted line) with a heating rate of 1.0 °C/min. The enzyme concentration was 0.14 mg/mL in 50 mM Tris-HCl, 1 mM EDTA, and 100 mM NaCl, pH 7.5

papain, and thiolsubtilisin (*9*). The p$K_a$ of 8.86 is also characteristic of a thiol group.

*Kinetic Deuterium Isotope Effects*. The alternative mechanism to the ion-pair formation may be the general base catalysis, which proceeds in deuterium oxide slower by a factor of 2−3, as found, in fact, with serine proteinases, but not with papain, whose thiolate-imidazolium ion-pair is well established (*9*). In the reaction of picornain 2A, the slight inverse kinetic deuterium isotope effect failed to support general base catalysis as the potential rate determining step, but it was consistent with ion-pair formation (*11*). Similar results were obtained with PV3C (Figure 1b), indicating practically identical changes in the two limiting rate constants (Table 1, column A/B). However, the absence of a normal kinetic deuterium isotope effect ($k(H_2O/k^2H_2O$ of 2−3) does not rule out general base catalysis. For example, a rate-limiting conformational change may mask general base catalysis (*19*, *20*).

Acylation characterized by $k_{cat}/K_m$ is a more complicated reaction compared with the simple nucleophilic alkylation, since its reaction involves a tetrahedral intermediate which is stabilized by hydrogen bonds from the oxyanion binding site, and may thus exhibit different isotope effects. Therefore, we have examined the kinetic deuterium isotope effects in a real catalytic process, by using fluorogenic substrate and by measuring the pH dependence of $k_{cat}/K_m$ in water and heavy water. With PV3C(M27G) this provided a much greater inverse effect (2.5-fold higher in heavy water), than that obtained in the alkylation reaction (Figure 3). Interestingly, the catalytically competent pH range was much broader with the 3C enzyme than with picornain 2A (*11*), but the isotope effects were similar (0.41 and 0.37 for picornains 3C and 2A, respectively). Picornains thus differ both from papain which does not show a kinetic deuterium isotope effect, and from chymotrypsin which exhibits isotope effects typical for general base catalysis. It should be noted that inverse deuterium isotope effects has already been observed with papain, but the values were much less pronounced (*21*−*23*) than those found here. Great inverse effects, comparable to those found here, were obtained with glucokinase. The large effects were interpreted either that two free enzyme forms interconverted with an altered rate in deuterium oxide or that the substrate affinity of the two forms altered with changing solvent (*24*).

The interpretation of solvent isotope effects on enzyme-catalyzed reactions not always straightforward. Thus, deuterium oxide may also modify the stability of the protein structure (*25*), which in turn can significantly influence the catalytic efficacy. This is indeed the case with picornains. The stabilization effect of heavy water is clearly shown by comparing the denaturation rates of picornains in urea dissolved in water or in deuterium oxide, assuming that the more stable structure denatures more slowly. We have fluorometrically monitored the denaturation processes, which followed first-order decays in 4.8 M urea. The denaturation rate indeed slowed in deuterium oxide as the rate constant decreased with PV3C(M27G) from 0.20 ± 0.01 $min^{-1}$ to 0.025 ± 0.001 $min^{-1}$.

DSC proved to be another helpful method for probing the stability of picornains in deuterium oxide. As shown in Figure 4, there is a substantial increase in the melting point of PV3C(M27G) in $^2H_2O$, which amounts to 11.8 °C, changing from 48.0 °C to 59.8 °C. There is also a significant, though smaller, shift associated with HRV2 2A (not shown).

*Thermodynamic Parameters*. Going from the ground state to the transition state of the reaction, the reactants become more ordered because a number of translational and rotational degrees of freedom of motion will be frozen. This implies that the activation entropy of the reaction ($\Delta S^*$) should be negative, provided that other factors do not interfere with the entropy change. It follows then that a loose, more flexible structure may have a greater change in $\Delta S^*$ during the reaction. Should the structural flexibility of PV3C be catalytically important, its looser structure in water would show a more negative $\Delta S^*$ than does the more stable species in deuterium oxide.

Figure 5 shows the Eyring plots for the reactions of PV3C in water and deuterium oxide. It is seen that the curves are not linear over the entire temperature range. There is a break in linearity well below the physiological temperature and the melting point determined with DSC. The break starts at

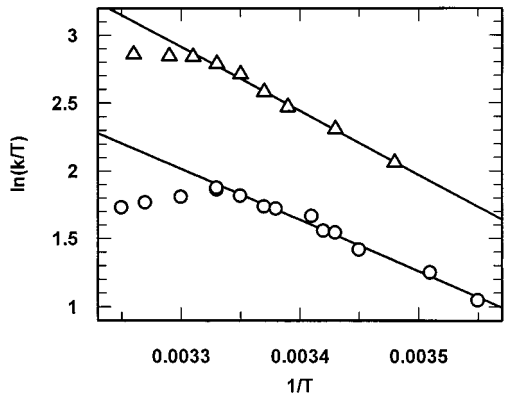


FIGURE 5: Eyring plots for picornain 3C measured with Abz-Glu-Ala-Leu-Phe-Gln-Gly-Pro-Phe($NO_2$)-Ala substrate. The reactions were carried out at pH 7.6 in water (○) and deuterium oxide (△).

lower temperature (~27 °C) in water than in deuterium oxide (~29 °C), which is consistent with the above finding that PV3C is more stable in deuterium oxide than in water. The difference is even more emphasized by the quality of change, as at high temperature the slope related to $\Delta H^*$ becomes less negative in heavy water, but the negative value changes to positive in water, which suggests that a change in the reaction mechanism occurs with increasing temperature, most interestingly close to the physiological temperature. It should be pointed out that in water the reduction in the rate constant does not stem from the denaturation of the protein since after incubation at 30 °C, the enzyme gives the same rate constant at 25 °C as measured without preincubation.

The thermodynamic parameters for the picornain 3C reaction could readily be calculated from the linear portion of the Eyring plots of Figure 5. The results indicate that the hydrolysis of the oligopeptide substrate has a more negative $\Delta S^*$ in water ($-77.0$ J mol$^{-1}$ K$^{-1}$) than in deuterium oxide ($-44.1$ J mol$^{-1}$ K$^{-1}$). This is consistent with the stability measurements, according to which the enzyme is more stable and more active in deuterium oxide. Apparently, it is more difficult for the less ordered active site in water to reach the ordered transition state.

*Conclusions*. It is generally accepted that the active sites of cysteine peptidases contain a thiolate-imidazolium ion-pair, which exists in a broad pH-range and accounts for the nucleophilic reactivity of the catalytically competent cysteine residue. However, experimental evidence for the existence of such ion-pairs has only been offered in the case of papain and thiolsubtilisin. An alternative way of assistance by the catalytic histidine involves general base catalysis, as found with serine peptidases having a related mechanism. Picornains and serine peptidases share the preference for an acidic amino acid (aspartic or glutamic acids) in the catalytic triad. The charged residue should stabilize the ion-pair of picornain better than the asparagine of the enzymes of the papain family. However, here we have clearly demonstrated that PV3C(M27G) does not have a catalytically competent ion-pair, and so the mechanism of the histidine assistance may be general base catalysis. Unfortunately, the kinetic deuterium isotope effect, which is not a straightforward method, could not be utilized for directly demonstrate general base catalysis.

## REFERENCES

1. Krausslich, H.-G., and Wimmer, E. (1988) *Ann. Rev. Biochem. 57*, 701−754.
2. Skern, T., and Liebig, H.-D. (1994) *Methods Enzymol. 244*, 583−595.
3. Ryan, M. D., and Flint, M. (1997) *J. Gen. Virol. 78*, 699−723.
4. Bergmann, E. M., and James, M. N. G. (1999) in *Proteases of infectious agents* (Dunn, B. M., Ed.) pp 139−163, Academic Press, London.
5. Allaire, M., Cherney, M. M., Malcolm, A. and James, M. N. G. (1994) *Nature (London) 369*, 72−76.
6. Matthews, D. A., Smith, W. W., Ferre, R. A. Condon, B., Budahazi, G., Sisson, W., Villafranca, J. E., Janson, C. A., McElroy, H. E., Gribskov, C. L., and Worland, S. (1994) *Cell 77*, 761−771.
7. Mosimann, S. C., Cherney, M. M., Sia, S., Plotch, S., and James, M., N., G. (1997) *J. Mol. Biol. 273*, 1032−1047.
8. Petersen, J. F. W., Cherney, M. M., Liebig, H.-D., Skern, T., Kuechler, E., and James, M. N. G. (1999) *EMBO J. 18*, 5463−5475.
9. Polgár, L. (1974) *FEBS Lett. 47*, 15−18.
10. Polgár, L. (1989) *Mechanisms of protease action*, pp 123−125, CRC Press, Boca Raton, FL.
11. Sárkány, Z., Skern, T., and Polgár, L. (2000) *FEBS Lett. 481*, 289−292.
12. Polgár, L. (1974) *FEBS Lett. 38*, 187−190.
13. Ivanoff, L. A., Towatari, T., Jasodhara, R., Korant, B. D., and Petteway, S. R., Jr. (1986) *Proc. Natl. Acad. Sci. U.S.A. 83*, 5382−5396.
14. Polgár, L, Erdélyi, F., Hajnal, É., Löw, M., Gráf, L., and Korant, B. D. (1993) *Biochem. J. 290*, 797−800.
15. Nicklin, M. J. H., Harris, K. S., Pallai, P. V., and Wimmer, E. (1988) *J. Virol. 62*, 4586−4593.
16. Ellman, G. L. (1959) *Arch. Biochem. Biophys. 82*, 70−77.
17. Leatherbarrow, R. J. (1998) *GraFit*, Version 4, Erythacus Software Ltd., Staines.
18. Glassoe, P. K., and Long, F. A. (1960) *J. Phys. Chem. 64*, 188−190.
19. Polgár, L. (1992) *Biochem. J. 283*, 647−648.
20. Polgár, L., Kollát, E., and Hollósi, M. (1993) *FEBS Lett. 322*, 227−230.
21. Polgár, L. (1979) *Eur. J. Biochem. 98*, 369−374.
22. Brocklehurst, K., Kowlessur, D., Patel, G., Templeton, W., Quigley, K., Thomas, E. W., Wharton, C. W., Wilenbrock, F., and Szawelski, R. J. (1988) *Biochem. J. 250*, 761−772.
23. Wandinger, A., and Creighton, D. J. (1980) *FEBS Lett. 116*, 116−121.
24. Pollard-Knight, D., and Cornish-Bowden, A. (1984) *Eur. J. Biochem. 141*, 157−163.
25. Huyghues-Despointes, B. M. P., Scholtz, J. M., and Pace, C. N. (1999) *Nat. Struct. Biol. 6*, 910−912.

BI010550P